



Tadpole morphological characterization of *Ranitomeya variabilis* (Zimmermann & Zimmermann, 1988) (Anura: Dendrobatidae), with skeleton, muscle system and inner organs

Ruth A. Regnet^{1,2} · Paul Lukas³ · Dennis Rödder^{1,2} · Benjamin Wipfler¹ · Mirco Solé^{1,2}

Received: 16 May 2023 / Revised: 8 August 2023 / Accepted: 11 August 2023 / Published online: 12 September 2023
© The Author(s) 2023

Abstract

In this study, we morphologically examine larval specimens of *Ranitomeya variabilis*, which were bred in captivity and genetically determined to belong to the French Guiana population. We provide detailed data on the external morphology, chondrocranium, cranial muscle systems and inner organs of the tadpoles. Additionally, we provide essential characteristics for the recognition of the tadpoles of the different *Ranitomeya* species. The external morphology of the *R. variabilis* tadpoles was assessed by measurements and photographs of the specimens. Internal morphology was analyzed using μ CT images, μ CT-based three-dimensional reconstructions, and dissection of specimens for organ and muscle descriptions. The majority of the muscle configurations observed herein for larval specimens of *R. variabilis* are consistent with data presented in previous studies for larvae of other *Ranitomeya* species. In addition, several of the observed morphological characters are defined for different taxonomic levels within Dendrobatidae, e.g., the reduction of tectal cartilages and the insertion of the M. rectus cervicis on the third or fourth branchial arch. The absence of the anterolateral process of the ceratohyal in *Ranitomeya* and *Dendrobates* further strengthens their close relationship, in contrast to the more distantly related *Epipedobates* and *Phylllobates* where this structure is present. The absence of the M. levator arcuum branchialium I and II, the M. interhyoideus posterior and the M. diaphragmatopraecordialis might be defining traits for *Ranitomeya*. The specific characters observed in this study for *R. variabilis*, are the fusion of the superficialis and profundus portion of the musculus levator longus larvae and the absence of the parotic crista.

Keywords Chondrocranium · Dendrobatidae · French Guiana · Larva · μ -CT scans

Introduction

The family Dendrobatidae Cope, 1865 (1850) is distributed exclusively in South and Central America. It currently comprises 205 neotropical frog species (Frost et al. 2022) and this number tends to increase due to cryptic species. In the last 16 years, special attention has been paid to the

phylogeny of this group. A redefinition has been proposed and part of it has been elevated to the superfamily Dendrobatoidea, including two families. New genera have been proposed and several new species have been described (Grant et al. 2006; Santos et al. 2009; Brown et al. 2011). Currently the family comprises 16 genera: *Adelphobates*, *Ameerega*, *Andinobates*, *Colostethus*, *Dendrobates*, *Ectopoglossus*, *Epipedobates*, *Excidobates*, *Hyloxalus*, *Leucostethus*, *Minyobates*, *Oophaga*, *Paruwrobates*, *Phylllobates*, *Ranitomeya* and *Silverstoneia* (Frost 2022). Dendrobatids frogs are characterized by a wide variety of colors and morphotypes, skin toxins, elaborate reproductive behavior and a complex and diverse parental care (Lötters et al. 2007; Poelman and Dicke 2007; Brown et al. 2011; Sánchez 2013). They back riding tadpoles present characteristically an oval body shape and brown to black–brown coloration (Lescure and Bechter 1982; Brown et al. 2011; Sanches 2013; Krings et al. 2017; Klein et al. 2020). However, morphological data

✉ Ruth A. Regnet
regnet_ruth@hotmail.com

¹ Leibniz-Institut zur Analyse des Biodiversitätswandels (LIB), Zoologisches Forschungsmuseum Alexander Koenig, Adenauerallee 127, 53113 Bonn, Germany
² Programa de Pós-Graduação em Zoologia, Universidade Estadual de Santa Cruz - UESC, Rodovia Jorge Amado, Km 16, Salobrinho, Ilhéus, Bahia 45662-900, Brazil
³ Institut für Zoologie und Evolutionsforschung, Friedrich-Schiller-Universität, Erbertstr. 1, 07743 Jena, Germany

including detailed descriptions of inner organs are scarce for tadpoles of this group, and only a few studies have addressed this topic (e.g., Brown et al. 2011; Sánchez 2013; Krings et al. 2017). The main reason for the lack of information may be the difficulty in obtaining an appropriate number of specimens in adequate development stages, as example in this study, were the sample size is only five specimens. The majority of tadpoles studied in this group is collected from the males' back and are newly hatched (Brown et al. 2011).

Within the genus *Ranitomeya*, the Zimmermann's Poison Frog, *R. variabilis* (Zimmermann and Zimmermann 1988; Fig. 1) is listed as data deficient in the Red List of Threatened Species (IUCN 2022). This species is diurnal and has a promiscuous mating strategy (Brown et al. 2011; Muell et al. 2022). Clutches are deposited directly on phytotelma, with 1–6 eggs deposited slightly above the waterline (Poelman and Dicke 2007). Males of this species provide parental care for eggs, embryos and tadpoles, and transport tadpoles to developmental sites (Lötters et al. 2007; Poelman and Dicke 2007; Brown et al. 2011).

Like in other dendrobatid species, *R. variabilis* has often been synonymized with other species (see Frost 2022) and confused with its closely related sister species *R. amazonica* (e.g., Brown et al. 2011), which is the only further representative of the *R. variabilis* species group. Recently, *Ranitomeya* populations from French Guiana and Brazil, previously reported as *R. amazonica*, were now related to *R. variabilis* (Brown et al. 2011; Muell et al. 2022). A reflection of the species synonymisation is the confusion on natural history data between species. For example, a cannibalistic strategy of *R. variabilis* tadpoles and on conspecific eggs has been described under the synonym *Dendrobates ventrimaculatus* Shreve, 1935 (Poelman and Dicke 2007). Observations of the breeding behavior of *R. variabilis* in captivity have also been described under the synonym *D. quinquevittatus* (Steindachner 1864), (see Lescure and Bechter 1982) and subsequently related to *R. amazonica* (Brown et al. 2011). A brief review on the external morphology of the larval stages 25–26 was provided by Masche et al. (2010). The description of a stage 27 tadpole as defined by Gosner (1960) and



Fig. 1 Adult individual of *Ranitomeya variabilis*, genetically assigned to the population from French Guiana, from the institutional breeding facility of the Zoological Research Museum Alexander Koenig (ZFMK), Germany, Bonn

the mouth of a stage 38 tadpole can be found under the synonym of *Dendrobates quinquevittatus* (Lescure and Bechter 1982). However, probably due to the synonymisation of the species, the language of the study being in French and due to the fact that the periodic from 1982 is not easily accessible, this study seems to have been largely overlooked.

Here, we examine tadpole specimens of *R. variabilis*, which are genetically determined to belong to the population from French Guiana, providing detailed data on the external morphology, the chondrocranium, the cranial muscle systems and the inner organs to guide the correct identification of *R. variabilis* larva in the field. We also compare existing data on the larval morphology of *Ranitomeya* with new additional morphological data of *R. variabilis* obtained in this study.

Material and methods

We analyzed five captive-bred tadpoles of *R. variabilis* in developmental stages 40 ($n=4$) and 38 ($n=1$) according to Gosner (1960). All tadpoles are deposited under the voucher numbers ZFMK 104000–104004 in the Herpetological Collection of the Leibniz-Institut zur Analyse des Biodiversitätswandels (LIB), Zoological Research Museum Alexander Koenig (ZFMK) and were collected from the institutional breeding facility of the ZFMK. The specimens were fixed in PFA 40% and stored in 80% ethanol. The species was identified by comparing the external morphology of adult specimens with descriptions for the specimens of the French Guiana population (Lescure and Bechter 1982; Brown et al. 2011; Muell et al. 2022) and by DNA barcoding, GenBank accession numbers OQ547269–OQ547270 (Regnet et al. 2023). Sequences were obtained from two additional larval specimens and were compared to 168 *Ranitomeya* species sequences available in GenBank (Regnet et al. 2023).

The morphology of the *R. variabilis* tadpoles was assessed by measurements, photographs and illustrations of the specimens. For the external morphology, all measurements were performed on the five tadpoles (ZFMK 104000–104004) before other techniques were applied (Table 1). Internal morphology was analyzed using μ CT images, μ CT-based three-dimensional reconstructions, and by direct observation under stereomicroscope. For this purpose, one tadpole (ZFMK 104001) was cleared and stained to extract cartilage and bone data; one (ZFMK104000) was dissected to obtain organ and muscle data, and one specimen (ZFMK 104003) was critical point dried for μ CT scans.

External morphological measurements

Measurements were taken through a stereomicroscope with integrated millimeter ruler (Stemi 2000 C; Carl Zeiss®

Table 1 External morphological character measurements of the *Ranitomaya variabilis* tadpoles, in developmental stages (stg) 38 ($n=1$) and 40 ($n=4$) of Gosner. Values expressed in mm and presented in Mean, Standard Deviation, Maximum and Minimum. Traits abbreviations are fully spelled in the methodology section

Traits	Mean	Std	Max	Min
TL	25.58	2.64	29.40	22.50
BL	9.32	0.44	10.00	8.80
TaL	16.26	2.33	19.40	13.20
BHE	5.82	0.70	7.00	5.30
BHN	3.36	0.70	4.10	2.20
MBH	7.56	0.69	8.40	6.80
TMW	2.24	0.33	2.60	1.90
IOD	3.22	0.27	3.50	2.80
IND	1.74	0.11	1.90	1.60
MBH	4.87	0.63	5.50	3.80
MTaH	3.92	0.52	4.70	3.50
TaMH	1.66	0.40	2.30	1.20
TfU	1.66	0.11	1.80	1.50
TfL	1.04	0.09	1.20	1.00
RED	2.80	0.24	3.10	2.50
END	1.68	0.13	1.80	1.50
RND	1.14	0.19	1.40	1.00
RSD	6.16	0.77	7.50	5.50
ND	0.18	0.03	0.20	0.15
SL	0.64	0.09	0.80	0.60
ED	0.86	0.13	1.00	0.70
ODW	2.14	0.15	2.40	2.00

Microscopy GmbH, Jena, Germany) according to Altig and McDiarmid (1999), Grosjean (2005) and Klein et al. (2022). The following abbreviations were used for the morphological terms: Dorsal view: body length (BL), body width on the eyes (BWE), body width on the nostril (BWN), eye diameter (ED), internarial distance (IND), interorbital distance (IOD), tail length (TaL), tail muscle width at base (TMW) and total length (TL). Lateral view: body height on the eyes (BHE), body height on the nostril (BHN), maximum body height (MBH), maximum body width (MBW), eye–nostril distance (END), nostril diameter (ND), rostrum–eye distance (RED), rostrum–nostril distance (RND), rostrum–spiracle distance (RSD), spiracle length (SL), tail–fin height lower (TfL), tail–fin height upper (TfU), maximum tail height (MTaH) and tail muscle height at base (TaMH). Ventral view: oral disc width (ODW). Photographs were taken using a Canon digital camera (EOS 600D; Canon® Deutschland GMBH, Krefeld, Germany) attached to a stereomicroscope.

Clearing and staining

We used the protocol for differential staining of cartilage and bone in whole formalin-fixed vertebrates (Wassersug

1976), which was adapted for tadpoles as described in detail in Krings et al. (2017). The results on the morphology of bone and cartilaginous tissue obtained through the clearing and staining methodology were compared with the results obtained from μ CT reconstructions. After the procedure, the specimen was returned to the ZFMK collection.

Dissection

To prepare the tadpoles for dissection to access the muscles and main inner organs, the first steps of the clearing and staining protocol in Krings et al. (2017) were followed. The specimen was stained with Alcian blue to facilitate the visualization of internal structures. Staining with Alcian blue, 15 mg in 80 ml EtOH, was performed overnight. Posteriorly the specimens were washed three times with EtOH 99%, and subsequently in five descending EtOH series, from 99 to 30%, for 1–2 h each, the last one of 30% was kept overnight. The skin of the specimen can be easily removed after the application of a solution of 80% KOH and 20% H_2O_2 for 1–2 h. To obtain the largest possible number of post metamorphic data, we used the tadpole at the most advanced developmental stage for this methodology. The dissection also helps to corroborate the μ CT results on the cranial muscles of *R. variabilis* tadpoles. After this procedure, the specimen was returned to the ZFMK collection.

μ -CT scans and 3D reconstruction

For this purpose, the specimen ZFMK 104001 was critical point dried using a Leica EM CPD300, following Bray et al. (1993). Images were acquired using a SkyScan 1173 (Bruker microCT, Kontich, Belgium) software = version 1.6, hardware version = A. The source voltage was 45 kV and current 177 μ A. Pixel size was 8.87 μ m. The resolution of the scans used for additional measurements was 13.19 μ m and the number of rows was 2240. The raw data were reconstructed using NRecon (version 1.7.5.9, Bruker microCT, SkyScan, Kontich, Belgium). To reconstruct the chondrocranium, cranial muscles and ossification from the μ CT-scans, a segmentation of the different skeletal structures was performed in Amira 6.0.1. 3D analysis software (FEI Visualization Sciences Group). Polygonal surfaces were rendered and then exported in the Wavefront OBJ file format for further processing in Autodesk Maya 2020 (Autodesk, Inc.). Surfaces were smoothed, polygonal counts reduced, and the surfaces arranged. For the final composition and rendering of images, Autodesk Mudbox 2020 (Autodesk, Inc.) was used. After this procedure, the specimen was replaced in alcohol 80% and also returned to the ZFMK collection.

Results

External larval morphology

The description is based on a single specimen of *R. variabilis* (ZFMK 104002) at stage 38 (Fig. 2) and we matched the morphological characters with the other four specimens studied herein. The described specimen shows a body wrinkled skin due to the fixing process. All measurements are given in millimeters.

Dorsal view: The body shape of the tadpole is classified as rounded according to morphogeometric standardization proposal of Dubeux et al. (2020). In lateral view, the tadpole is narrower (MBW 8.4 mm) in relation to its body length (BL 10.0 mm). The distance between the eyes is larger than the distance between the nostrils (IOD 3.4 and IND 1.9 mm). The spiracle, nostril openings and the mouth are not visible in dorsal view.

Lateral view: The body is depressed, with maximum body height just posterior to the eyes (MBH 5.0 mm). The snout is short and rounded (RED 3.0 and RND 1.0 mm). Eyes (ED 0.8 mm) and the nostrils (ND 0.2 mm) are dorsal and have a lateral orientation, the elliptical shape of the nostrils only are noticed on the lateral view. The nostrils are closer to the snout (RND 1.4 mm) than to the eyes (END 1.8 mm). Due to a skin fold, that connects the anterior edge of the eyes and the nostril, its opening and shape is only observed in lateral



Fig. 2 *Ranitomeya variabilis* tadpole, on development stage 38 of Gosner (1960), fixed in formalin 40% and preserved in alcohol 80% (ZFMK 104003). Scale bar 2 mm

view. The spiracle is sinistral and positioned ventrolaterally at the posterior half of the body (RSD 7.5 mm), the opening is round and the spiracle tube is short (SL 0.8 mm). The tail is narrower in relation to the maximum body width (MTH 4.7 mm) and ends in a rounded shape. The caudal musculature is robust (TMH 2.3 mm), the "V"-shaped myoseptae are visible along the entire length of the caudal musculature, which gradually narrows posteriorly and ends before the end of the tail, which consists only of the tail fin. The tail fins present different maximum heights (TfU 1.8 and TfL 1.2 mm) and both expand posteriorly to the tail-body junction, the lower fin being slightly anterior to the upper fin. The oral apparatus is visible in lateral view and a lateral-line system is not evident.

Ventral view: The ventrally located oral disc has an elliptical and laterally emarginated shape (ODV 2.4 mm, Fig. 3). The oral disc is bordered by a row of rounded papillae. These are present on the posterior labium and on the sides of the upper labium, the submarginal papillae form a small cluster near the corners of the lateral disc. The remaining anterior labium lacks papillae. Both jaw sheaths are black and serrated, while the upper being wider than the lower. The upper labium possesses two tooth rows. The first tooth row is continuous, although in some specimens analyzed herein, some denticles in the row were missing, forming small gaps on the tooth rows, as if it were a sequence of dashed lines, but clearly not divided into two or three tooth rows. The first row has longer teeth than the second. The second upper row is divided into two parts, placed laterally in the labium and widely separated from each other. The lower labium possesses three tooth rows. The first is divided medially, with a smaller distance compared to the upper second row. While the second and third are continuous, the third being a little thinner, there are gaps present in some of the herein studied specimens. The labial tooth row formula is 2(2)/3(1). The ventral tube, with elliptical opening, is dextral and emerges sagittally from the abdomen. Hindlimbs are not fully developed and the metatarsal tubercle, typical for the stage 38 of

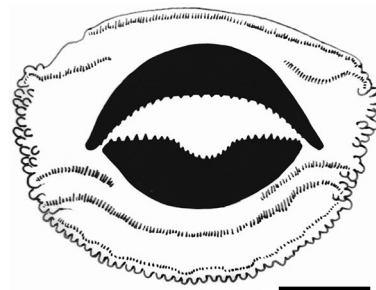


Fig. 3 *Ranitomeya variabilis* oral disc representation. Tadpole on development stage 38 of Gosner (1960). Scale bar 0.5 mm

Gosner (1960), can already be observed. The ventral body skin is not translucent, but in some specimens, it may be slightly transparent. In some cases, a part of the intestine or developing forelimbs can be observed through the skin.

Colouration of a preserved tadpole in stage 38: The ground color is gray–brown except for two lighter patches, with a beige–brown hue, anterior to the eyes and situated below the eyes on the outside of the nostrils, but not including the nostrils. In addition, the tail muscle and the attachment of the tail muscle to the body are more distinct. The dorsum in general has a darker gray–brown color in relation to the ventral region and hind limbs. The tail, including the transparent fin, is beige–brown and the edge of the tail fin is lighter. The eyes are grey with white pupils and the jaw sheaths and tooth rows are black.

Colouration of a living tadpole in stage 38: The base color of the tadpole is brown to black–brown, and the eyes are black (Fig. 4). At this developmental stage, the dorsum is partially colored in a species-specific manner. A yellow mosaic can be seen, mainly between the eyes and the nostrils, which extends along the dorsum. At the plane of the eyes, the mosaic proceeds in two lateral lines until the midline of the body and is gradually lost posteriorly. In the center of the dorsum, a third and lighter line, but not yellow colored, can be observed. In the first half of the body, mainly concentrated in the region between the eyes and the mouth, several small blue–metallic and yellow dots can be observed, but they are not clearly visible without magnification. The ventral side, as well as, the hind limbs, is completely brown to black–brown and the fingers are grey, and their tips are translucent. The tail fins are beige and transparent.

Larval internal morphology

Descriptions are based on specimens ZFMK 104000, 104001 and 104,003 of *R. variabilis* tadpoles.

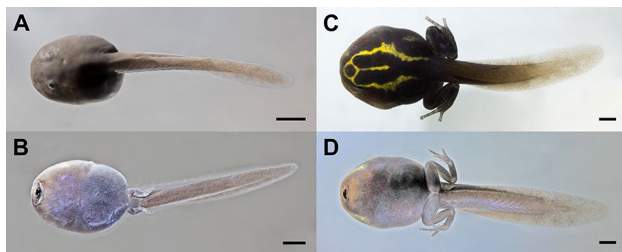


Fig. 4 *Ranitomeya variabilis* tadpole in life. A: development stage 30 of Gosner (1960) in dorsal view, B: development stage 35 in ventral view, C: development stage 41 in dorsal view and D: development stage 41 in ventral view. Scale bar 2 mm

Dissection: In ventral view (Figs. 5 and 6), the intestine, which occupies the largest portion of the body cavity, is coiled sinistrally. In the central part of the intestinal spiral, the coiling direction changes. The liver and gallbladder are located on the right side of the body and are partially covered by the intestine. The pancreas is located in the center of the body cavity, to the left of the oesophagus. The front legs, which were still under the skin inside the body cavity, are now visible and are fully formed. The heart is located between the two front legs. Additionally, different muscles of the head can be seen in the specimen, in ventral and dorsal views, these are detailed in Fig. 7.

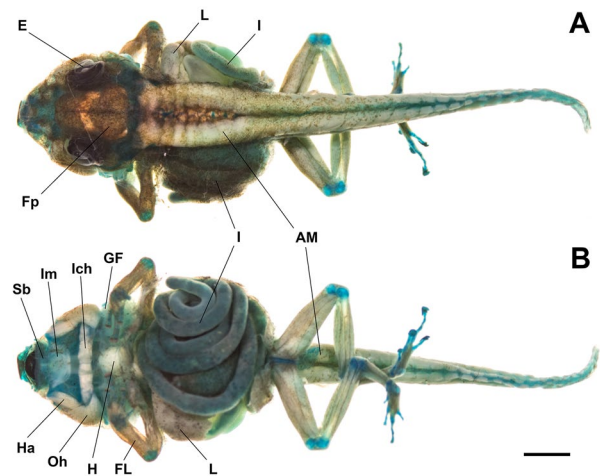


Fig. 5 Dissected specimen of *Ranitomeya variabilis* on development stage 40 of Gosner (1960). Ventral view of the specimen ZFMK 104000, stained with alcian blue and skinned. Scale bar 2 mm. A dorsal and B ventral view. Abbreviations: AM axial musculature, E Eye, FL frontal limb (was still in the corporeal cavity), Fp frontoparietale, GF gill filaments, H heart, HA hyoangularis, I intestine, Ich interhyoideus, Im intermandibularis, L Liver, Oh orbitohyoideus, Sb submentalis

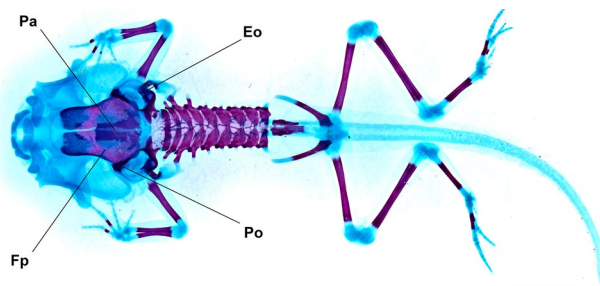


Fig. 6 Dorsal view of the complete skeleton *Ranitomeya variabilis*, at development stage 40 of Gosner (1960). Clearing and staining procedure of the specimen ZFMK 104001, cartilage tissue shown in blue and ossifications in purpura. Scale bar 2 mm. Abbreviations: Eo exoccipitale, Fp frontoparietale, Pa parasphenoid, Po prootic

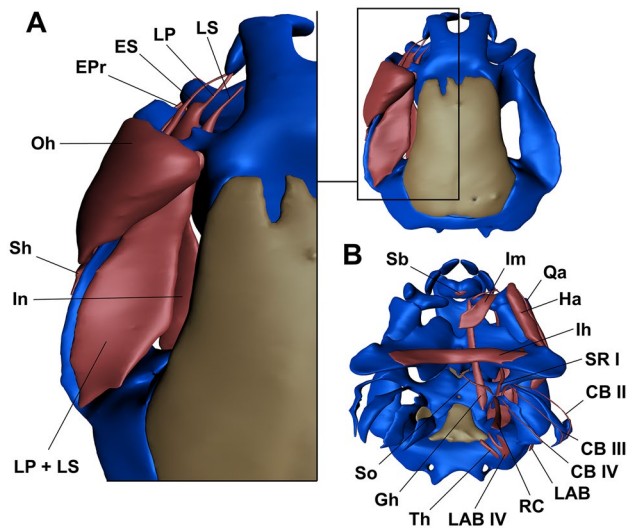


Fig. 7 Condocranial muscles (purpura coloration) of *Ranitomeya variabilis* tadpole at development stage 40 of Gosner (1960). Amira Micro-CT scan reconstruction procedure of the specimen ZFMK 104003. In dorsal (A) and ventral (B) views. Ossifications shown in brown and cartilage tissue in blue. Abbreviations: Cb: constrictor branchialis II–IV, EPr: externus profundus, ES: externus superficialis, Gh: geniohyoideus, Ha: hyoangularis, Ih: interhyoideus, Im: intermandibularis, In: internus, LAB: levator arcuum branchialium III, LAB: levator arcuum branchialium IV, LP: longus profundus, LS: longus superficialis, MI: mandibulolabialis, Qa: quadratoangularis, RC: rectus cervicis, Oh: orbitohyoideus, Sb: submental, SH: suspensoriohyoideus, SO: subarcualis obliquus, SR: subarcualis rectus I, Th: tympanopharyngeus

Chondrocranium morphology: The following description is based on specimens at Gosner stage 40 (Fig. 7A, B, Fig. 8A–D). The suprarostril cartilage is quadripartite. The suprarostril plate is medially separated and consists of two medial bodies. Both parts of the suprarostril plate are laterally bordered by square-shaped alae. Each suprarostril ala bears one posterior process on its posterodorsal surface. Both, the suprarostril alae and the two bodies of the suprarostril plate, articulate dorsally with the trabecular horns. Adrostril and admandibular cartilages are absent. The infrastril cartilage is single and runs horizontally. Its mediolateral surface is connected to the rounded anterior tip of each Meckel's cartilage via the intramandibular joint. Meckel's cartilage is paired and sigmoid, with the anterodorsal surface bearing the intramandibular joint. The retroarticular process lies posteroventrally and surrounds the articular process of the palatoquadrate ventrally. The jaw joint is hinge like and preorbital.

The palatoquadrate is broad, plate-like and laterally adjacent to the neurocranium. It connects the viscerocranial and neurocranial derivatives of the larval head skeleton. The articular process is present at the anterior margin. It is a short and broad process which dorsally borders the retroarticular process of Meckel's cartilage. The

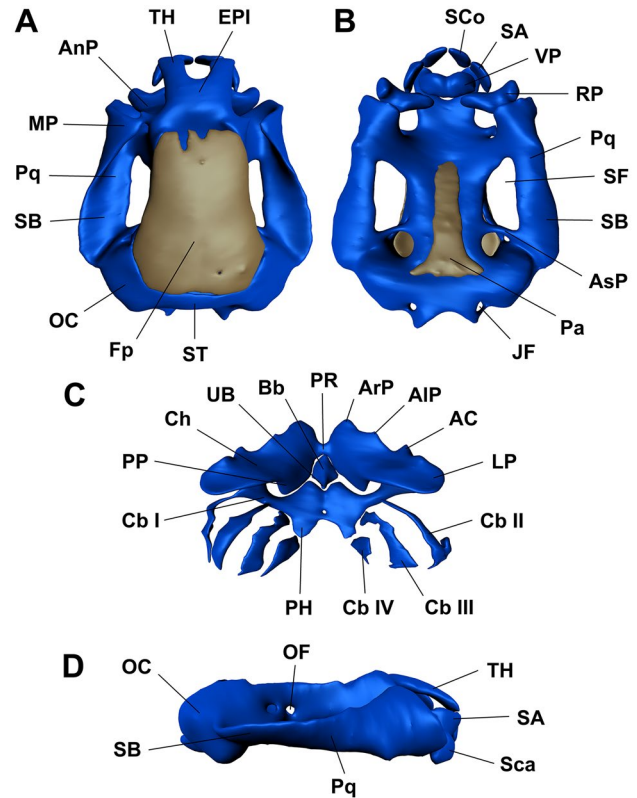


Fig. 8 Chondrocranium and frontoparietalia of a *Ranitomeya variabilis* tadpole at development stage 40 of Gosner (1960). Dorsal (A) and ventral (B) views, as well as, the branchial arch (C) and the cranial lateral view (D) of the specimen ZFMK 104003. Ossifications shown in brown and cartilage tissue in blue. Abbreviations: AC: articular condyle, AIP: anterolateral process, AnP: antorbital process, ArP: anterior process, AsP: ascending process, Bb: basibranchial, Cb: ceratobranchial (I–IV), Ch: ceratohyal, EPI: ethmoid plate, Fp: frontoparietal, HP: hypobranchial plate, JF: jugular foramen, LP: lateral process, MP: muscular process, OC: otic capsule, OF: oculomotor foramen, Pa: parasphenoid, PP: posterior process, Pq: palatoquadrate, PR: pars reuniens, RP: retroarticular process, SA: suprarostril ala, SB: subocular bar, Sca: meckel's cartilage, SCo: suprarostril corpus, SF: subocular fenestra, ST: synotic tectum, TH: trabecular horns, UB: urobranchial process and VP: ventromedial process

anterolateral border of the palatoquadrate is formed by the dorsomedially projecting and triangular shaped muscular process. The process almost reaches the dorsal tip of the lateral brain wall. The quadratoethmoidal process and the pseudopterygoid process are absent. Posteriorly a broad, horizontal subocular bar emerges. The lateral margin is slightly curved laterally. Posteriorly the curvature of the subocular bar is concave with a bulging margin. The palatoquadrate is connected to the otic capsule via a broad otic process. At the posteromedial margin of the palatoquadrate the ascending process emerges anterodorsally at an angle of 45° and connects the palatoquadrate to the lateral brain wall. The curvature of the posterior part of the palatoquadrate extends into the lateral space of the

otic capsule. A larval otic process is absent. The basihyal is absent. The ceratohyal is a single cartilage and its distal tips protrude beyond the lateral margin of the palatoquadrate. The lateral parts of the ceratohyal are joined medially by a chondrified pars reuniens. The medial part of the ceratohyal is horizontally oriented whereas the lateral parts are twisted vertically. The anterior margin is curved and bears two processes, a triangular anterolateral and a rounded anterior process. The lateral process is broad, rounded and plate-like. The postcondylar process extends far dorsally and is triangular. The posterior process is short and pointed. The basibranchial is free, of triangular shape, and bears a posteriorly proceeding, long, and pointed urobranchial process.

The trabecular horns are connected to the ethmoid plate posteriorly and bordered by the suprarostal cartilage anteriorly. Their width is uniform and they proceed only slightly oblique. The ethmoid plate is longer than the trabecular horns and is confluent with the basicranial floor and the orbital cartilage. The anterior part of the lateral brain wall bears a pointed antorbital process. Tectal cartilages are missing or inconspicuous. The basicranial fenestra is already closed, the optic and oculomotor foramen are present at the posterior part of the lateral brainwall. The otic capsules reach about 25% of the total length of the chondrocranium and bear no parotic crista. The posterodorsal parts of the capsules are connected via a broad synotic tectum. The brain is covered dorsally by a single, plate-like frontoparietal. A T-shaped parasphenoid is present beneath the ventral margin of the basicranial floor.

Mandibular, hyoid, branchial and hypobranchial musculature: We identified a total of 22 muscles in the tadpole of *R. variabilis* (origins and insertions are given in Table 2, Fig. 7 A–B). The *M. mandibulolabialis* consists of a single slip inserting at the lower lip and the *M. intermandibularis* is U-shaped. The *M. levators mandibulae longus superficialis* and *M. mandibulae longus* are fused at their origin but the muscle ends in two long tendons. The *M. subarcualis rectus* only consists of one slip. *M. levators arcuum branchialium I* and *II* are absent. The anterior margin of the hypobranchial plate is broad and rounded. Both plates connect each other in their anterior two thirds. The posterior part is less wide and proceeds posterolaterally. All terminal and proximal commissures are absent. Ceratobranchial I is arched from the anterolateral margin of the hypobranchial plate. The lateral part of ceratobranchial I is plate-like. Ceratobranchials II–IV are not connected to the hypobranchial plate or to each other. They are also arcuate. Ceratobranchial II is the longest and ceratobranchial IV is the shortest one. All ceratobranchials lack spicules and processes.

Discussion

Here, we present a detailed morphological description of captive-bred tadpoles of *R. variabilis* from French Guiana. We want to emphasize the current importance of studies on captive-bred amphibian species. Due to the life history of this group, obtaining amphibian larvae in the natural environment at developmental stages necessary for a morphological study is by nature a complex task. In addition, the current decline in amphibian populations has increased the difficulty in obtaining natural environment data for these specimens. Furthermore, frog populations are not only declining but also entirely disappearing from many natural areas (Gascon et al. 2007).

The rounded body shape of the *R. variabilis* tadpoles studied here, as well as their brown to black–brown coloration in life seem to be a common and easily confused feature of *Ranitomeya* tadpoles (Lescure and Bechter 1982; Brown et al. 2011; Sanches 2013; Krings et al. 2017; Klein et al. 2020). The main differences detected herein between the tadpoles of the different species of *Ranitomeya* are the small morphological traits (Table 3). Such as the measurement values of the eye–nostril distance (END), internarial distance (IND), rostrum–eye distance (RED) as well as, rostrum–spiracle distance (RSD), that show higher for *R. variabilis*. Due to the general morphological similarity of the *Ranitomeya* tadpoles, these morphological characteristics could be relevant characters for the recognition of the larva of these species. Nevertheless, we emphasize that the present study, and the studies with tadpoles of *Ranitomeya* that have been referred to as references here, are based on tiny specimen samples. Therefore, additional research would be ideal to confirm whether these traits can actually be used to distinguish between tadpoles of different *Ranitomeya* species.

Two chondrocranial characters are defining characters for the Dendrobatidae (Haas 2003). Both the reduction of tectal cartilages and the insertion of the *M. rectus cervicis* on the third or fourth branchial arch are present in *R. variabilis*, which further strengthens these characters as defining ones. Additionally, the *M. levator mandibulae externus superficialis* is missing in the *R. variabilis* tadpole examined at stage 40. This feature has been described previously as characteristic of dendrobatids (Myers et al. 1991). The quadripartite suprarostal observed in *R. variabilis* with independent left and right parts of the suprarostal corpus and independent left and right suprarostal alae can be observed in other dendrobatids as well. Similar to other investigated species of *Ranitomeya*, the four parts of the suprarostal in *R. variabilis* are separated by symphyses (Krings et al. 2017). In later stages of *Epipedobates* and *Dendrobates*, the left and the right parts of the suprarostal

Table 2 Mandibular, hyoid, branchial and hypobranchial musculature of *Ranitomeya variabilis* tadpoles in development stage 40 of Gosner (1960)

Muscle	Origin	Insertion	Comments
<i>Mandibular arch muscles</i>			
Lev. mand. longus superficialis	Caudodorsal surface of the subocular cartilage	Mediodorsal surface of meckel's cartilage; caudal surface of suprarostril ala	Superficialis and longus portion fused at origin
Lev. mand. internus	Ventral surface of ascending process	Dorsolateral surface of meckel's cartilage,	Ends in a long tendon
Lev. mand. externus superficialis	Medial, inferior surface of muscular process (superior)	Laterodorsal tip of meckel's cartilage	
Lev. mand. externus profundus	Medial, inferior surface of muscular process (medial)	Caudovernal surface of suprarostril ala	
Mandibulolabialis	Ventromedian surface of meckel's cartilage	Lower lip	
<i>Hyoid arch muscles</i>			
Hyoangularis	Anterior surface of the lateral process of ceratohyal	Lateral surface of retroarticular process of meckel's cartilage	
Suspensorioangularis	Caudovernal surface of subocular cartilage	Lateral surface of retroarticular process of meckel's cartilage	
Orbitohyoideus	Lateral surface of muscular process	Ventrolateral surface of ceratohyal	
Suspensoriohyoideus	Caudolateral surface of muscular process	Anterovernal surface of subocular cartilage	
Intermandibularis posterior	Caudomedial surface of meckel's cartilage,	Median raphe	
Interhyoideus	Ventrolateral surface of ceratohyal	Median raphe	
<i>Branchial arch muscles</i>			
L. arc. branchialium III	Lateral margin of otic capsule	Caudolateral surface of ceratobranchial iii	
L. arc. branchialium IV	Caudolateral margin of otic capsule	Caudolateral surface of ceratobranchial iv	
Constr. branchialis II	Lateral surface of ceratobranchial ii	Anteromedial part of ceratobranchial ii	
Constr. branchialis III	Lateral surface of ceratobranchial ii	Caudomedial part of ceratobranchial ii	
Constr. branchialis IV	Lateral surface of ceratobranchial iii	Caudomedial part of ceratobranchial iii	
Subarcualis rectus I	Anterior surface of ceratobranchial iii	Caudal surface of ceratohyal	
Subarcualis rectus II–IV	Anterior surface of ceratobranchial iii	Anterior surface of ceratobranchial ii	
Subarcualis obliquus II	Anterior surface of ceratobranchial iii	Urobranchial process of basibranchial	
<i>Hypobranchial muscles</i>			
Geniohyoideus	Ventral surface of hyobranchial plate	Caudolateral surface of infrarostril cartilage	
Rectus cervicis	Peritoneum	Medial surface of ceratobranchial iii	

corpus fuse (Haas 1995). A missing adrostril cartilage can be confirmed in the genus *Ranitomeya*. It is also missing in *Dendrobates*, whereas it is present in *Colostethus*, *Epipedobates* and *Phylllobates* (Haas 1995). The posterior curvature of the palatoquadrate of *R. variabilis* is similar to other investigated species of *Ranitomeya* (Krings et al. 2017). The curvature is high and overlaps laterally with the anterior half of the otic capsule. The contact between the curvature and the otic capsule is broad and the ascending process is less obvious than in *Epipedobates anthonyi* (Haas 1995). The larval otic process is missing in *R. variabilis* and in all dendrobatids investigated so far. The anterolateral process of the ceratohyal is missing in *R.*

variabilis as described for other species of *Dendrobates* and *Ranitomeya* (Krings et al. 2017; Haas 1995; De Sá and Hill 1998). It is present in *Epipedobates* and *Phylllobates* (Haas 1995). A parotic crista was described in *Ranitomeya* before (Krings et al. 2017), in *R. variabilis* no such structure was observed. This may be a character that distinguishes *R. variabilis* from other *Ranitomeya* species. Further studies are needed to corroborate this trait and to exclude observational errors and methodological limitations.

The majority of muscle configurations are consistent with previous studies on *Ranitomeya* tadpoles. The M. levatores arcuum branchialium I and II, the M. interhyoideus posterior

Table 3 Comparison of the morphometric characters from different *Ranitomeya* species

Traits	<i>R. variabilis</i>	<i>R. amazonica</i>	<i>R. benedicta</i>	<i>R. imitator</i>	<i>R. reticulata</i>	<i>R. sirensis</i>	<i>R. vanzolinii</i>
TL	25.98	27.67	28.67	26.84	22.17	18.47	25.86
BL	9.32	9.38	9.38	9.69	8.38	6.37	9.00
TaL	16.26	18.29	19.29	17.14	13.79	12.10	16.86
BWE	5.82	5.57	5.00	5.29	4.58	4.33	4.86
BWN	3.36	3.14	2.86	3.43	2.96	3.83	3.14
MBW	7.56	7.00	7.29	7.14	5.16	5.47	6.86
TMW	2.24	2.29	2.43	2.29	1.87	1.60	2.29
IOD	3.22	3.00	3.57	3.29	2.93	1.74	3.29
IND	1.74	1.57	1.43	1.43	1.57	1.05	1.57
MBH	4.87	4.14	4.29	5.15	3.48	3.87	4.86
MTH	3.92	3.71	4.14	4.43	3.07	3.30	4.00
TMH	1.66	2.14	2.57	2.43	1.64	1.69	2.14
RED	2.80	2.15	1.69	2.08	1.79	1.55	2.08
END	1.68	1.23	1.00	1.08	1.20	1.06	1.31
RND	1.14	0.92	0.69	1.00	2.37	0.49	0.77
RSD	6.16	6.00	5.23	5.92	5.38	3.40	5.46
ED	0.86	1.13	1.00	0.74	0.80	0.55	0.86
ODW	2.14	1.86	2.14	2.14	2.04	2.12	1.86

Values expressed in mm. *R. variabilis* (present study), mean values of Gosner developmental stages (stg) 38 ($n=1$) and 40 ($n=4$). Data for *R. amazonica* (stg 41, $n=1$), *R. benedicta* (stg 41, $n=1$), *R. imitator* (stg 41, $n=1$), *R. reticulata* (stg 41, $n=1$), *R. sirensis* (stg 29, $n=1$) and *R. vanzolinii* (stg 41, $n=1$), are adapted from Klein et al. (2020). Traits abbreviations are fully spelled in the methodology section

and the M. diaphragmatopraecordialis are absent in *R. variabilis* as well as in other investigated species of *Ranitomeya* (Krings et al. 2017). But some features are unique to *R. variabilis* such as the absence of the M. quadratoangularis. The M. subarcualis rectus I only possess one instead of two portions. The origin and the insertion of the M. subarcualis rectus II-IV which runs from the anterior surface of ceratobranchial III to the anterior surface of ceratobranchial II is similar to the condition found in *R. vanzolinii* and *R. imitator* (Krings et al. 2017). This distinguished these three species from *R. amazonica* and *R. benedicta* where the M. subarcualis rectus II-IV runs from ceratobranchial IV to ceratobranchial III.

Conclusion

The morphological data generated here for *R. variabilis* show that the external morphological characteristics of *Ranitomeya* tadpoles is very similar. Thus, perhaps the quantitative data can shed some light on the differentiation of these species as larger samples are studied. We have also shown that several morphological characters are defining for different taxonomic levels within dendrobatids. For example, the reduction of tectal cartilages and the insertion of the M. rectus cervicis on the third or fourth branchial arch are defining traits for Dendrobatids. The absence of the anterolateral process of the ceratohyal in *Ranitomeya* and *Dendrobates*

further strengthens their close relationship, in contrast to the more distantly related *Epipedobates* and *Phylllobates* where this structure is present. The absence of the M. levator arcuum branchialium I and II, the M. interhyoideus posterior and the M. diaphragmatopraecordialis might be defining traits for *Ranitomeya*, and a unique feature of *R. variabilis* in comparison to other *Ranitomeya* species is the absence of the parotic crista.

Acknowledgements We thank Juliane Vehof, for help with the μ CT scans and for the assistance in the morphological laboratory. Morris Flecks, Rafid AlKhalidi and Ursula Bott for helping with the preparation of the figures. Daniel Loebmann, Denise Rossa-Feres, Etielle Andrade, Renan N. Costa and anonymous reviewers for reviewing the manuscript. Ruth A. Regnet acknowledges the Coordenação de Aperfeiçoamento de Pessoal de Nível Superior (CAPES) for granting a doctoral scholarship (88882.451536/2019-01). Mirco Solé acknowledges funding by Conselho Nacional de Desenvolvimento Científico e Tecnológico (CNPq, productivity grant 309365/2019-8) and by Coordenação de Aperfeiçoamento de Pessoal de Nível Superior (CAPES) and Alexander von Humboldt Foundation (BEX 0585/16-5). Paul Lukas acknowledges funding by the Deutsche Forschungsgemeinschaft (DFG; LU 2404/1-1).

Author contributions RAR, PL, BW, DR, MS: Conceptualization, Methodology. RAR, PL: Data curation, Writing- Original draft preparation. RAR, PL, DR: Visualization, Investigation. DR, MS: Supervision. RAR, PL, DR, MS: Writing- Reviewing and Editing

Funding Open Access funding enabled and organized by Projekt DEAL. Coordenação de Aperfeiçoamento de Pessoal de Nível Superior, 88882.451536/2019-01, Deutsche Forschungsgemeinschaft, LU

2404/1-1, Conselho Nacional de Desenvolvimento Científico e Tecnológico, 309365/2019-8, Capes/Humboldt, BEX 0585/15-5

Declarations

Conflict of interest The authors declare no competing interest.

Open Access This article is licensed under a Creative Commons Attribution 4.0 International License, which permits use, sharing, adaptation, distribution and reproduction in any medium or format, as long as you give appropriate credit to the original author(s) and the source, provide a link to the Creative Commons licence, and indicate if changes were made. The images or other third party material in this article are included in the article's Creative Commons licence, unless indicated otherwise in a credit line to the material. If material is not included in the article's Creative Commons licence and your intended use is not permitted by statutory regulation or exceeds the permitted use, you will need to obtain permission directly from the copyright holder. To view a copy of this licence, visit <http://creativecommons.org/licenses/by/4.0/>.

References

- Altig R, McDiarmid RW (2007) Morphological diversity and evolution of egg and clutch structure in amphibians. *Herp Monogr* 21:1–32. <https://doi.org/10.1655/06-005.1>
- Bray DF, Bagu J, Koegler P (1993) Comparison of hexamethyldisilazane (HMDS), Peldri II, and critical point drying methods for scanning electron microscopy of biological specimens. *Microsc Res Tech* 26:489–495. <https://doi.org/10.1002/jemt.1070260603>
- Brown JL, Twomey E, Amézquita A, de Souza MB, Caldwell JP, Lötters S, von May R, Melo-Sampaio PR, Mejía-Vargas D, Pérez-Peña PE, Pepper M, Poelman EH, Sanchez-Rodriguez M, Summers K (2011) A taxonomic revision of the Neotropical Poison frog genus *Ranitomeya* (Amphibia: Dendrobatidae). *Zootaxa* 3083:1–120
- Gascon C, Collins JP, Moore RD, Church DR, McKay JE, Mendelson JR III (eds) (2007) Amphibian Conservation Action Plan. IUCN/SSC Amphibian Specialist Group. Gland, Switzerland and Cambridge, UK.
- De Sá RO, Hill S (1998) Chondrocranial anatomy and skeletogenesis in *Dendrobates auratus*. *J Herpetol* 32:205–210
- Dubeux MJM, Nascimento FACD, Lima LR, Magalhães FDM, Silva IRS, Gonçalves U, Almeida JPF, Correia LL, Garda AA, Mesquita DO, Rossa-Feres DC, Mott T (2020) Morphological characterization and taxonomic key of tadpoles (Amphibia: Anura) from the northern region of the Atlantic Forest. *Biota Neotrop* 20:1–24
- Frost DR (2021) Amphibian Species of the World: an Online Reference. Version 6.1 (06 Mai 2022). Electronic Database accessible at <https://amphibiansoftheworld.amnh.org/index.php>. American Museum of Natural History, New York, USA. <https://doi.org/10.5531/db.vz.0001>. Accessed 6 May 2022.
- Gosner KL (1960) A simplified table for staging anuran embryos and larvae with notes on identification. *Herpetol* 16:183–190
- Grant T, Frost DR, Caldwell JP, Gagliardo R, Haddad CFB, Kok PJR, Means DB, Noonan BP, Schargel WE, Wheeler W (2006) Phylogenetic systematics of dart-poison frogs and their relatives (Amphibia: Athesphatanura: Dendrobatidae). *Bull Am Mus Nat* 299:1–262
- Haas A (1995) Cranial features of dendrobatid larvae (Amphibia: Anura: Dendrobatidae). *J Morphol* 224:241–264. <https://doi.org/10.1002/jmor.1052240302>. (PMID: 7595955)
- Haas A (2003) Phylogeny of frogs as inferred from primarily larval characters (Amphibia: Anura). *Cladistics* 19:23–89
- IUCN 2022. The IUCN Red List of Threatened Species. Version 2021–3 (06 Mai 2022). <https://www.iucnredlist.org>. Accessed 6 May 2022.
- Klein B, Regnet RA, Krings M, Rödder D (2020) Larval development and morphology of six Neotropical poison-dart frogs of the genus *Ranitomeya* (Anura: Dendrobatidae) based on captive-raised specimens. *Bonn Zool Bull* 69:191–223
- Koch C, Venegas PJ, Rödder D, Flecks M, Böhme W (2013) Two new endemic species of *Ameiva* (Squamata: Teiidae) from the dry forest of northwestern Peru and additional information on *Ameiva concolor* Ruthven, 1924. *Zootaxa* 3745:263–295
- Krings M, Klein B, Heneka MJ, Rödder D (2017). Morphological comparison of five species of poison dart frogs of the genus *Ranitomeya* (Anura: Dendrobatidae) including the skeleton, the muscle system and inner organs. *PLoS ONE* 12: e0171669. doi:<https://doi.org/10.1371/journal.pone.0171669>
- Lescure J, Bechter R (1982) Le comportement de reproduction en captivité et le polymorphisme de *Dendrobates quinquevittatus* Steindachner (Amphibia, Anura, Dendrobatidae). *Rev Fr Aquar - Herp* 8:107–118
- Lötters S, Jungfer K, Henkel FW, Schmidt W (2007) Poison frogs. Biology, species and captive husbandry. Edition Chimaira, Frankfurt am Main.
- Masche S, Zimmermann H, Pröhl H (2010) Description and Ecological Observations of the Tadpole of *Ranitomeya variabilis* (Anura: Dendrobatidae). *S Am J Herpetol* 5:207–211. <https://doi.org/10.2994/057.005.0306>
- Muell MR, Chávez G, Prates I, Guillory WX, Kahn TR, Twomey EM, Rodrigues MT, Brown JL (2022) Phylogenomic analysis of evolutionary relationships in *Ranitomeya* poison frogs (Family Dendrobatidae) using ultraconserved elements. *Mol Phyl Evol* 168:107389
- Myers CW, Paolillio OA, Daly JW (1991) Discovery of a defensively malodorous and nocturnal frog in the family Dendrobatidae: phylogenetic significance of a new genus and species from the Venezuelan Andes. *Am Mus Novit* 3002:1–33
- Poelman EH, Dicke M (2007) Offering offspring as food to cannibals: oviposition strategies of Amazonian Poison frogs (*Dendrobates ventrimaculatus*). *Evol Ecol* 21: 215–227.
- Regnet RA, Rech I, Rödder D, Solé M (2023): Captive Breeding, Embryonic and Larval Development of the Zimmermann's Poison-Frog *Ranitomeya variabilis* (Zimmermann & Zimmermann, 1988), (Anura: Dendrobatidae). *ZooKeys* 1172: 131–153.
- Sánchez DA (2013) Larval morphology of Dart-Poison frogs (Anura: Dendrobatoidea: Aromobatidae and Dendrobatidae). *Zootaxa* 3637:569–591
- Santos JC, Coloma LA, Summers K, Caldwell JP, Ree R (2009) Amazonian amphibian diversity is primarily derived from late Miocene Andean lineages. *PLoS Biol*, 7(3), e1000056. <http://dx.doi.org/https://doi.org/10.1371/journal.pbio.1000056>
- Steindachner F (1864) Batrachologische Mittheilungen. *Verh Zool Bot Ver Wien* 14(239–288):260–261
- Wassersug R (1976) A procedure for differential staining of cartilage and bone in whole formalin-fixed vertebrates. *Stain Techn* 51:131–134
- Zimmermann H, Zimmermann E (1988) Etho-Taxonomie und zoogeographische Artengruppenbildung bei Pfeilgiftfröschen (Anura: Dendrobatidae). *Salamandra* 24:125–160

Publisher's Note Springer Nature remains neutral with regard to jurisdictional claims in published maps and institutional affiliations.